Version 02 as of January 2, 2020
Primary authors: Carlos Yero, Werner Boeglin, Mark Jones
To be submitted to PRL
Comment to cyero002@fiu.edu by xxx, yyy

First Measurements of the D(e,e'p)n Cross Section at Very High Recoil Momenta and Large Q^2

C. Yero and W.U. Boeglin
Florida International University, University Park, Florida 33199, USA

M.K. Jones
Thomas Jefferson National Accelerator Facility, Newport News, Virginia 23606, USA

(for the Hall C Collaboration)
(Dated: January 2, 2020)

New $^2H(e,e'p)n$ cross sections have been measured at 4-momentum transfers of $Q^2 = 4.5 \pm 0.5$ $(\mathrm{GeV/c})^2$ reaching neutron recoil (missing) momenta up $p_r \sim 1.18$ GeV/c. The data have been obtained at fixed neutron recoil angles (θ_{nq}) of 35° and 45° with respect to the 3-momentum transfer, $\vec{q}$. At these kinematic settings final state interactions (FSIs), meson exchange currents (MECs) and isobar configurations (ICs) are expected to be suppressed and the plane wave impulse approximation (PWIA) provides the dominant cross section contribution. The new data are compared to recent theoretical calculations where a significant disagreement at very high missing momenta has been observed.

The deuteron is the only two-nucleon bound system. Therefore, it serves as a starting point to study the strong nuclear force at the subfermi distance scale, a region which is currently not well understood. At such small internucleon distances the NN (nucleon-nucleon) potential is expected to exhibit a repulsive core in which the interacting nucleon pair begins to overlap. The overlap is directly related to two-nucleon short range correlations (SRC) observed in $A > 2$ nuclei [1–4]. Short-range studies of the deuteron are also important in determining whether or to what extent the description of nuclei in terms of nucleon/meson degrees of freedom is still valid before having to include explicit quark degree of freedoms, an issue of fundamental importance in nuclear physics[5]. As of the present time, there are only a few nuclear physics experiments for which a transition between nucleonic to quark degrees of freedom been observed [6–8].

The most direct way to study the short range structure of the deuteron wavefunction (or equivalently, its high momentum components) is via the exclusive deuteron electro-disintegration reaction at very high neutron recoil (or missing) momenta. Within the PWIA, the virtual photon couples to the proton which is subsequently ejected from the nucleus without further interaction with the recoiling neutron. The neutron carries a momentum equal in magnitude but opposite in direction to the initial state proton, $\vec{p}_r = -\vec{p}_{i,p}$, thus providing information on the momentum of the bound nucleon and its momentum distribution.

In reality, the ejected particles undergo subsequent interactions resulting in re-scattering between the proton and neutron (FSIs). Another possibility is that the photon may couple to the virtual meson being exchanged between the nucleons (MECs), or the photon may excite either nucleon in the deuteron into a resonance state (ICs) which decays back into the ground state nucleon causing further re-scattering between the proton and neutron. Both MECs and ICs in addition to FSIs can significantly alter the recoiling neutron momentum thereby obscuring any possibility of directly accessing the deuteron momentum distributions.

Theoretically, MECs and ICs are expected to be suppressed at $Q^2 > 1$ $(\mathrm{GeV/c})^2$) and Bjorken $x_{Bj} \equiv Q^2/2M_p\omega > 1$, where M_p and ω are the proton mass and photon energy transfer, respectively. The suppression of MECs can be understood from the fact that the estimated MEC scattering amplitude is proportional to $(1+Q^2/m^2_{meson})^{-2}(1+Q^2/\Lambda^2)^{-2}$, where $m_{meson} \approx 0.71$ $(\mathrm{GeV/c})^2$ and $\Lambda^2 \sim 0.8-1$ $(\mathrm{GeV/c})^2$[9]. The ICs can be suppressed kinematically by selecting $x_{Bj} > 1$, where one probes the lower part of the deuteron quasi-elastic peak which is maximally away from the inelastic resonance electro-production threshold.

For FSIs at large Q^2, the onset of the General Eikonal Approximation (GEA)[9–11] is expected which predicts a strong angular dependence of the FSIs with neutron recoil angles where FSI peaks at $\theta_{nq} \sim 70^o$. The most important prediction from GEA, however, is that at large recoil momenta p_r where FSIs are expected to be large, there is an approximate cancellation of the PWIA/FSI interference (screening term) with the modulus-squared of

the FSI amplitude (rescattering term). This cancellation results in only the PWIA term remaining in the deuteron cross section and is expected to occur at netron recoil angles $\theta_{nq} \sim 40^o$ and $\theta_{nq} \sim 120^o$. Since at $\theta_{nq} \sim 120^o$ ICs are not negligible, $x_{Bj} > 1$ is required to suppress ICs which leaves $\theta_{nq} \sim 40^o$ as the only choice where FSIs are reduced.

Previous deuteron electro-disintegration experiments performed at Jefferson Lab (JLab) have helped confirmed various of the abovementioned theoretical predictions as well as constrain and quantify the contributions from FSIs, MECs and ICs on the $^2H(e,e'p)n$ cross-section to determine the kinematics at which they are either suppressed (MECs and ICs) or under control (FSIs). The first of these was performed in Hall A [12] at a relatively low momentum transfer of $Q^2 = 0.665$ (GeV/c)^2 and neutron recoil momenta up to $p_r = 550$ MeV/c where it was shown that for $p_r > 300$ MeV/c, FSIs, MECs and ICs dominate the cross section and had to be included in Arenhövel's calculations [13–16] for a satisfactory agreement between theory and data.

The next experiment was performed in Hall B [17] using the CEBAF Large Acceptance Spectrometer (CLAS) which measured a wide variety of kinematic settings giving an overview of the $^2H(e,e'p)n$ reaction kinematics. This was the first experiment to probe the deuteron at high momentum transfers ($1.75 \leq Q^2 \leq 5.5$ (GeV/c)^2) and presented angular distributions of cross-sections that exhibited a strong angular dependence of FSI with neutron recoil angles peaking at $\theta_{nq} \sim 70^o$ which confirmed the onset of the GEA[9, 10]. The cross sections versus neutron recoil momenta up to p_r ~2 GeV/c were also presented, however, statistical limitations made it necessary to integrate over a wide angular range making it impossible to control contributions from FSIs, MECs and ICs.

Finally, a third $^2H(e,e'p)n$ experiment was performed in Hall A [18] at $Q^2 = 3.5 \pm 0.25$ (GeV/c)^2 and recoil momenta up to 550 MeV/c. The angular distributions of the cross-section ratio ($R = \sigma_{exp}/\sigma_{PWIA}$) presented saw agreement in shape with the angular distributions in Hall B[17] with FSI peaking at $\theta_{nq} \sim 70^o$. With the increased statistics in Hall A, a direct comparison of the momentum distributions between data and theory could be made for specific θ_{nq} bins. For the first time, at $\theta_{nq} = 35 \pm 5^o$ and 45 ± 5^o, theoretical models showed a sensitivity to the NN-potential used in the deuteron wavefunction that was not obscured by FSI contributions to the cross section data.

The experiment presented in this Letter takes advantage of the kinematic window previously found in Hall A[18] and extends the $^2H(e,e'p)n$ cross section measurements to $Q^2 = 4.5 \pm 0.5$ (GeV/c)^2 and neutron recoil momenta up to 1.18 GeV/c. At these kinematics, MECs and ICs are suppressed and FSIs are under control for neutron recoil angles between 35 and 45 degrees giving access to unprecedented high momentum components of the deuteron wavefunction.

This experiment was part of a group of four experiments that commissioned the new Hall C Super High Momentum Spectrometer (SHMS) as part of the 12 GeV upgrade at JLab. A 10.6 GeV electron beam was incident on a 10 cm long liquid deuterium target (LD2). The scattered electron and knocked-out proton were detected in coincidence by the SHMS and the High Momentum Spectrometer (HMS), respectively. The "missing" (undetected) neutron was reconstructed from energy-momentum conservation laws: $\vec{p_r} = \vec{q} - \vec{p_f}$ (missing momentum) and $E_m = \omega - T_p - T_r$ (missing energy), where $\vec{p_f}$ is the final proton momentum, (T_p, T_r) are the final proton and neutron kinetic energies, and E_m is the binding (missing) energy of the deuteron. The beam currents delivered by the accelerator ranged between 45-60 μA and the beam was rastered over a 2x2 mm^2 area to reduce the effects of localized boiling on the cryogenic targets (hydrogen and deuterium).

Both spectrometers at Hall C have similar standard detector packages, each with 1) four scintillator planes[19] used for triggering, 2) a pair of drift chambers[20] used for tracking, 3) a calorimeter[21] used for e^-/π^- discrimination and 4) a gas Čerenkov [22, 23] used also for e^-/π^- separation. Due to the absence of significant background on this experiment and the low coincidence trigger rates ($\sim 1-3$ Hz) at the higher missing momentum settings, the use of additional particle identification (PID) was found to have little to no effect on the final cross section.

We measured three central missing momentum settings: $p_r = 80, 580$ and 750 MeV/c. At each of these settings, the electron arm (SHMS) was fixed and the proton arm (HMS) was rotated from smaller to larger angles corresponding the the lower and higher missing momentum settings, respectively. At these kinematics, the 3-momentum transfer covered a range of $2.4 \lesssim |\vec{q}| \lesssim 3.2$ GeV/c which is more than twice the highest neutron recoil momentum (p_r) measured on this experiment. As a result, most of the virtual photon momentum is transferred to the proton which scatters at angles relative to $\vec{q}$ in the range $0.4^o \lesssim \theta_{pq} \lesssim 21.4^o$. At these forward angles and large momentum transferred to the proton, the additional process in which the neutron is struck by the virtual photon is suppressed.

Hydrogen elastic $^1H(e,e'p)$ data was also taken at kinematics close to the deuteron p_r=80 MeV setting for cross-checks with the spectrometer acceptance model using the Hall C Monte Carlo simulation program, SIMC. Additional $^1H(e,e'p)$ data were also taken at three other kinematic settings that covered the SHMS momentum acceptance range for the deuteron and were used for spectrometer optics optimization, momentum calibration and the determination of the spectrometer offsets and kinematic uncertainties[24, 25].

Identical event selection criteria were used for the hy-

drogen and deuteron data. The criteria were determined by making 1) standard cuts on the spectrometer momentum fraction (δ) to select a region in which the reconstruction optics is well known, 2) a cut to restrict the HMS solid angle acceptance to events that passed directly through the collimator and not by re-scattering from the collimator edges, 3) a missing energy cut (peak $\sim$ 2.22 MeV for the deuteron) to select true $^2H(e,e'p)n$ coincidences, 4) a coincidence time cut to select true coincidence events and not accidentals, 5) a PID cut on the SHMS calorimeter to select electrons and not other sources of background, mostly pions and 6) a cut on the reconstructed HMS and SHMS reaction vertices to select events that truly originated from the same reaction vertex at the target.

The experimental data yield for both hydrogen and deuteron data was normalized by the total charge and corrected for various inefficiencies. For $^2H(e,e'p)n$ the corrections were as follows: tracking efficiencies (98.9%-HMS, 96.4%-SHMS), total live time (92.3%), proton loss due to nuclear interactions in the HMS (4.7%)[26] and target boiling factors (4.2%)[27].

For $^1H(e,e'p)$, the corrected data yield was compared to SIMC using J. Arrington's proton form factor parametrization[28] to check the spectrometer acceptance model. The ratio of data to simulation yield was determined to be $97.6 \pm 0.3\%$ (statistical uncertainty only). For $^2H(e,e'p)n$, the low missing momentum data ($p_r = 80$ MeV/c) were compared to the Hall A data (See Fig. 1). The good agreement gives us confidence on the measurements made at higher missing momentum settings for which no previous data exist.

The systematic uncertainties on the measured cross sections were determined from normalization[29] and kinematic uncertainties in the beam energy and spectrometer angle/momentum settings. The individual contributions from normalization uncertainties were determined to be: tracking efficiencies (0.40%-HMS, 0.59%-SHMS), target boiling (0.39%), total live time (3.0%) and total charge (2.0%) for an overall normalization uncertainty added in quadrature of 3.7%.

The systematic uncertainties due to our limited knowledge of the beam energy and spectrometer angle/momentum settings were determined point-to-point in (θ_{nq}, p_r) bins for each data set independently, and added in quadrature for overlapping p_r bins of different data sets. For $\theta_{nq} = 35$, 45 and 75 deg (presented on this Letter) the overall kinematic uncertainty varied up to 6.5% for $p_r \leq 1.01$ GeV/c. The overall systematic uncertainty in the cross section was determined by the quadrature sum of the normalization and kinematic uncertainties. This result was then added in quadrature to the statiscial uncertainty(25-30% on average) to obtain the final uncertainty in the cross section.

The data were radiatively corrected for each bin in (θ_{nq}, p_r) by multiplying measured cross sections to the ratio of the SIMC yield without and with radiative effects. For each bin in (θ_{nq}, p_r), the averaged $^2H(e,e'p)n$ kinematics has also been calculated and used in the bin centering correction factor defined as: $f_{bc} \equiv \sigma_{avg.kin}/\bar{\sigma}$, where $\sigma_{avg.kin}$ is the cross section calculated at the averaged kinematics and $\bar{\sigma}$ is the cross section averaged over the kinematic bin. The calculations were based on the Laget model including FSI[30, 31].

Both experimental and theoretical reduced cross sections were extracted from the measured (or model) cross

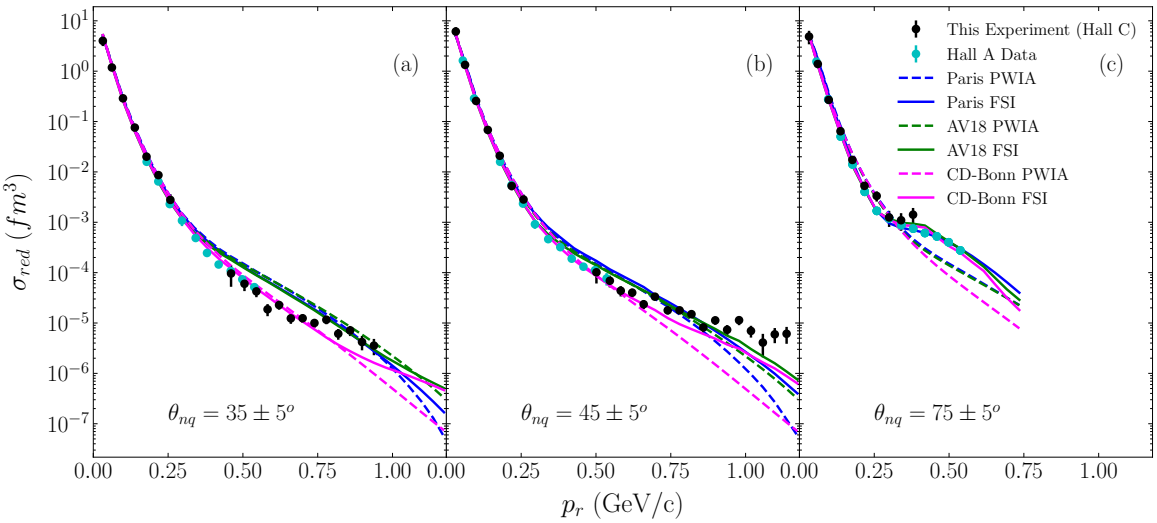

FIG. 1. The reduced cross sections $\sigma_{red}(p_r)$ as a function of neutron recoil momentum p_r are shown in (a)-(c) for recoil angles $\theta_{nq} = 35^o, 45^o$ and 75^o, respectively, with a bin width of $\pm 5^o$. The data is compared to the previous Hall A experiment (cyan) results[18] as well as the theoretical reduced cross sections using the Paris(blue), AV18(green) and CD-Bonn(magenta) NN potentials

sections for each data set independently and were averaged for overlapping bins in p_r. The reduced cross sections are defined as follows:

$$\sigma_{red} \equiv \frac{\sigma_{exp(th)}}{K f_{rec} \sigma_{cc1}} \quad (1)$$

where $\sigma_{exp(th)}$ is the 5-fold experimental (or theoretical) differential cross section $\frac{d^5\sigma}{d\omega d\Omega_e d\Omega_p}$, K is a kinematical factor, f_{rec} is the recoil factor that arises from the integration over missing energy and σ_{cc1} is the de Forest[32] electron-proton offshell cross section calculated using the form factor parametrization of Ref.[28]. Within the PWIA, σ_{red} corresponds to the proton momentum distribution inside the deuteron.

Figure 1 shows the extracted experimental and theoretical reduced cross sections as a function of neutron recoil momentum p_r for three angular settings at $Q^2 = 4.5 \pm 0.5$ (GeV/c)^2. The results from the previous Hall A experiment[18] at a $Q^2 = 3.5 \pm 0.25$ (GeV/c)^2 are plotted as well (cyan). The data is compared to theoretical reduced cross sections using the charge-dependent Bonn (CD-Bonn)[33], Argonne v_{18} (AV18)[34] and Paris[31] NN-potentials. The theoretical calculations for the CD-Bonn (magenta) and AV18 (green) potentials were performed by M. Sargsian[35] and those for the Paris (blue) potential were done by J.M. Laget[30].

At recoil angles $\theta_{nq} = 75^o$ [Fig. 1(c)], all models agree and are sensitive to momentum distributions up to p_r ~300 MeV/c. Beyond p_r ~300 MeV/c, FSIs become dominant and exhibit a similar behaviour among all models which obscures any possibility of extracting the momentum distributions at these angles. At smaller recoil angles, $\theta_{nq} = 35^o$ and 45^o [Figs. 1(a), 1(b)], the Paris and AV18 calculations show sensitivity to momentum distributions and are within good agreement whereas the CD-Bonn calculation exhibits a different behaviour beyond p_r ~300 MeV/c which indicates a larger sensitivity to the different NN-potentials at higher missing momenta.

The ratio of the experimental and theoretical reduced cross sections (σ_{red}) to the deuteron momentum distributions (n(p_r)) is shown in Fig. 2. As a reference we selected the deuteron momentum distribution calculated using the charge-dependent Bonn (CD-Bonn) potential[33].

At $\theta_{nq} = 75^o$ [Fig. 2(c)], there is a clear onset of GEA at $p_r \gtrsim 300$ MeV/c where FSI become dominant as indicated by the rise of FSI (solid lines) for all theoretical calculations as compared to the reference. In this region, our experiment is statistically limited as we focused on kinematics at lower recoil angles where FSIs are small. The overlayed Hall A data, however, shows excellent agreement with the Paris FSI. For $p_r < 300$ MeV/c, FSIs are small as indicated by the approximate ratio R~1 for all the theoretical calculations using FSI,

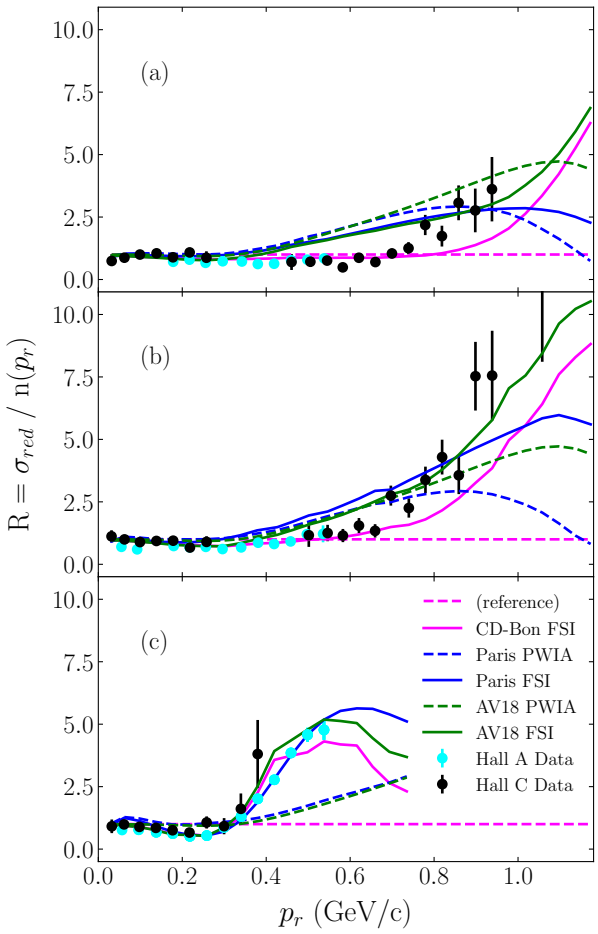

FIG. 2. The ratio R(p_r) = σ_{red}/n(p_r) is shown in (a)-(c) for $\theta_{nq} = 35^o, 45^o$ and 75^o, respectively, each with a bin width of $\pm 5^o$. The dashed reference (magenta) line refers to CD-Bonn momentum distribution (n(p_r)) by which the data and all models are divided.

which the data follows. The small dip observed in this region (R< 1) is indicative of the approximate (not exact) cancellation between the PWIA/FSI interference (screening term) and the modulus-squared of FSI (re-scattering) terms in the cross section.

For $\theta_{nq} = 45^o$ [Fig. 2(b)] at $p_r < 300$ MeV/c, all theoretical calculations agree with each other and are sensitive to the momentum distribution inside the deuteron which the data confirms. At $p_r \gtrsim 300$ MeV/c, the Paris/AV18 calculations start to deviate from the CD-Bonn calculations, with the most substantial deviations observed at $p_r \sim 1$ GeV/c. The CD-Bonn calculations are sensitive to momentum distributions up to p_r ~580 MeV/c before FSIs start to dominate (R> 1). The data agrees well with the CD-Bonn PWIA calculation but show an earlier rise than predicted by the CD-Bonn FSI, a behaviour which is not described by any of the models.

A similar behaviour is observed for $\theta_{nq} = 35^o$ [Fig. 2(a)], where the CD-Bonn calculations are sensitive to momentum distributions up to $p_r \sim 800$ MeV/c before being overwhelmed by FSIs, whereas the Paris/AV18 calculations start to deviate from the CD-Bonn at $p_r \sim 300$ MeV/c. The data shows sensitivity to CD-Bonn momentum distributions up to $p_r \sim$750 MeV/c before exhibiting an earlier rise than predicted by CD-Bonn FSI.

The $\theta_{nq} = 35^o$ [Fig. 2(a)] appears to be the optimal kinematics to study the high momentum components of the deuteron wavefunction, as the data is sensitive to momentum distributions up to $p_r \sim 750$ MeV/c as compared to $p_r \sim$580 MeV/c for the $\theta_{nq} = 45^o$ setting.

This experiment extended the previous Hall A cross section measurements on the $^2H(e, e'p)n$ reaction to unprecedented large Q^2 and very high neutron recoil momenta at kinematics that enhanced the high momentum components of the deuteron wavefunction. The experimental reduced cross sections were extracted and found to be in good agreement with the Hall A data. Furthermore, the CD-Bonn calculations were found to be sensitive to momentum distributions up to $p_r \sim 800$ MeV/c for recoil angles $\theta_{nq} = 35 \pm 5^o$, which the data agreed up to $p_r \sim 750$ MeV/c. At higher missing momentum, however, all models are unable to describe the data, which is currently not well understood.

Given that this was a commissioning experiment that ran for only 6 out of the 42 days (14.2%) of beam time and 3 out of the 8 original kinematic settings, additional beam time would be required to measure the full kinematic coverage (more missing momentum settings) to gain the necessary statistics in order to make any definitive arguments about the underlying physics observed.

We acknowledge the outstanding support of the staff of the Accelerator and Physics Divisions at Jefferson Lab as well as the entire Hall C staff, technicians, graduate students and users who took shifts or contributed to the equipment for the Hall C upgrade making all four commissioning experiments possible.

[1] K. S. Egiyan *et al.* (CLAS Collaboration), Observation of nuclear scaling in the $A(e, e')$ reaction at $x_B > 1$, Phys. Rev. C **68**, 014313 (2003).

[2] K. S. Egiyan *et al.* (CLAS Collaboration), Measurement of two- and three-nucleon short-range correlation probabilities in nuclei, Phys. Rev. Lett. **96**, 082501 (2006).

[3] R. Shneor *et al.* (Jefferson Lab Hall A Collaboration), Investigation of proton-proton short-range correlations via the $^{12}C(e, e'pp)$ reaction, Phys. Rev. Lett. **99**, 072501 (2007).

[4] N. Fomin, D. Higinbotham, M. Sargsian, and P. Solvignon, New results on short-range correlations in nuclei, Annual Review of Nuclear and Particle Science **67**, 129159 (2017).

[5] P. Ulmer *et al.*, Short-Distance Structure of the Deuteron and Reaction Dynamics in ^{2}H(e,e'p)n, https://www.jlab.org/exp_prog/proposals/01/PR01-020.pdf (2001), *Jefferson Lab Proposal E01-020*.

[6] C. Bochna *et al.*, Measurements of deuteron photodisintegration up to 4.0 gev, Phys. Rev. Lett. **81**, 4576 (1998).

[7] E. C. Schulte *et al.*, Measurement of the high energy two-body deuteron photodisintegration differential cross section, Phys. Rev. Lett. **87**, 102302 (2001).

[8] E. C. Schulte *et al.*, High energy angular distribution measurements of the exclusive deuteron photodisintegration reaction, Phys. Rev. C **66**, 042201 (2002).

[9] M. M. Sargsian, Selected Topics in High Energy Semi-Exclusive Electro-Nuclear Reactions, International Journal of Modern Physics E **10**, 405457 (2001).

[10] L. L. Frankfurt, M. M. Sargsian, and M. I. Strikman, Feynman graphs and generalized eikonal approach to high energy knock-out processes, Phys. Rev. C **56**, 1124 (1997).

[11] W. Boeglin and M. Sargsian, Modern studies of the deuteron: From the lab frame to the light front, International Journal of Modern Physics E **24**, 1530003 (2015), https://doi.org/10.1142/S0218301315300039.

[12] P. E. Ulmer *et al.*, ^{2}H$(e, e'p)n$ reaction at high recoil momenta, Phys. Rev. Lett. **89**, 062301 (2002).

[13] H. Arenhövel, W. Leidemann, and E. L. Tomusiak, Inclusive deuteron electrodisintegration with polarized electrons and a polarized target, Phys. Rev. C **43**, 1022 (1991).

[14] H. Arenhövel, W. Leidemann, and E. L. Tomusiak, Exclusive deuteron electrodisintegration with polarized electrons and a polarized target, Phys. Rev. C **46**, 455 (1992).

[15] H. Arenhövel, W. Leidemann, and E. L. Tomusiak, Nucleon polarization in exclusive deuteron electrodisintegration with polarized electrons and a polarized target, Phys. Rev. C **52**, 1232 (1995).

[16] H. Arenhövel, F. Ritz, H. Göller, and T. Wilbois, Consistent treatment of relativistic effects in electrodisintegration of the deuteron, Phys. Rev. C **55**, 2214 (1997).

[17] K. S. Egiyan *et al.* (CLAS Collaboration), Experimental study of exclusive ^{2}H$(e, e'p)n$ reaction mechanisms at high Q^2, Phys. Rev. Lett. **98**, 262502 (2007).

[18] W. U. Boeglin *et al.* (For the Hall A Collaboration), Probing the high momentum component of the deuteron at high Q^2, Phys. Rev. Lett. **107**, 262501 (2011).

[19] G. Niculescu, I. Niculescu, M. Burton, D. Coquelin, K. Nisson, and T. Jarell, Shms hodoscope scintillator detectors, https://hallcweb.jlab.org/document/howtos/shms_scintillator_hodoscope.pdf.

[20] M. Christy, P. Monaghan, N. Kalantarians, D. Biswas, and M. Long, Shms drift chambers, https://hallcweb.jlab.org/document/howtos/shms_drift_chambers.pdf.

[21] H. Mkrtchyan *et al.*, The lead-glass electromagnetic calorimeters for the magnetic spectrometers in hall c at jefferson lab, Nuclear Instruments and Methods in Physics Research Section A: Accelerators, Spectrometers, Detectors and Associated Equipment **719**, 85100 (2013).

[22] W. Li, *Heavy Gas Cherenkov Detector Construction for Hall C at Thomas Jefferson National Accelerator Facility*, Master's thesis, University of Regina (2012).

[23] D. Day, Preliminary design of the shms noble

cerenkov detector, https://hallcweb.jlab.org/DocDB/0009/000933/001/shms-cerv6.pdf.

[24] C. Yero, Update on spectrometer offsets determination using h(e,e'p) elastics (2019), https://hallcweb.jlab.org/DocDB/0010/001036/002/HC_SoftwareMeeting_Oct03_2019_pdf.pdf.

[25] C. Yero, Optics optimization for the d(e,e'p)n experiment [e12-10-003] (2019), https://hallcweb.jlab.org/DocDB/0010/001033/001/d2_optim.pdf.

[26] C. Yero, Proton absorption (2019), https://hallcweb.jlab.org/DocDB/0010/001020/002/ProtonAbsorption_slides.pdf.

[27] C. Yero, Hms target boiling studies (2019), https://hallcweb.jlab.org/DocDB/0010/001023/003/TargetBoiling_v2.pdf.

[28] J. Arrington, Implications of the discrepancy between proton form factor measurements, Phys. Rev. C **69**, 022201 (2004).

[29] Conservative estimates on the systematic uncertainties of the total live and charge were made. Determination of systematics on these quantities is a work in progress. (Private communication with D. Mack).

[30] J. Laget, The electro-disintegration of few body systems revisited, Physics Letters B **609**, 49 (2005).

[31] M. Lacombe, B. Loiseau, J. M. Richard, R. V. Mau, J. Côté, P. Pirès, and R. de Tourreil, Parametrization of the paris $n-n$ potential, Phys. Rev. C **21**, 861 (1980).

[32] T. D. Forest, Off-shell electron-nucleon cross sections: The impulse approximation, Nuclear Physics A **392**, 232 (1983).

[33] R. Machleidt, High-precision, charge-dependent bonn nucleon-nucleon potential, Phys. Rev. C **63**, 024001 (2001).

[34] R. B. Wiringa, V. G. J. Stoks, and R. Schiavilla, Accurate nucleon-nucleon potential with charge-independence breaking, Phys. Rev. C **51**, 38 (1995).

[35] M. M. Sargsian, Large Q^2 electrodisintegration of the deuteron in the virtual nucleon approximation, Phys. Rev. C **82**, 014612 (2010).

[36] W. U. Boeglin *et al.*, Deuteron Electro-Disintegration at Very High Missing Momenta, https://www.jlab.org/exp_prog/proposals/10/PR12-10-003.pdf.